

On the Birefringence of Multilayered Symmetric Diblock Copolymer Films

J. Kim,[†] I. Chin,[†] B. A. Smith, and T. P. Russell*

IBM Research Division, Almaden Research Center, 650 Harry Road,
San Jose, California 95120-6099

J. W. Mays

Department of Chemistry, University of Alabama at Birmingham,
Birmingham, Alabama 35294-1240

Received April 7, 1993; Revised Manuscript Received June 22, 1993*

ABSTRACT: The chain extension at lamellar interfaces was studied in thin films of symmetric diblock copolymers on gold substrates. The first copolymer consisted of blocks of polystyrene (PS) and poly(2-vinylpyridine) (P2VP), denoted P(S-*b*-2VP). The second was a diblock copolymer of PS and poly(methyl methacrylate) (PMMA), denoted P(S-*b*-MMA), on a gold substrate. Using attenuated total reflectance spectroscopy, the refractive indices parallel, n_{\parallel} , and perpendicular, n_{\perp} , to the surface of the films were determined. It was found that the total birefringence, $\Delta_T = n_{\perp} - n_{\parallel}$, of the as-cast films was positive, indicative of an orientation of the copolymer chains parallel to the film surface. Upon annealing at 170 °C, Δ_T changed sign and attained a limiting value, $\sim -7 \times 10^{-4}$ for P(S-*b*-2VP) and $\sim -20 \times 10^{-4}$ for P(S-*b*-MMA). It was found that the form birefringence, Δ_F , dominates the intrinsic birefringence, Δ_I , for P(S-*b*-MMA). On the other hand, Δ_I was much greater than Δ_F for P(S-*b*-2VP). From Δ_I the extension ratios of the chains at the interface were found to be 1.5–1.6 for both copolymers.

Introduction

The morphology of a microphase-separated diblock copolymer depends upon the volume fraction of the components comprising the blocks, the molecular weight of the copolymer, and the segmental interactions between the different components of the copolymer.¹ The size scale of the microdomains depends upon the minimization of the free energy which contains contributions from, among other things, the energy required to stretch the chains of each block at the interface so as to minimize contacts between the two different blocks. The extent to which the chains are stretched at the interface will dictate the variation in the periodicity of the microdomain morphology. For example, for symmetric diblock copolymers in the strong segregation limit, the radius of gyration of the chains, R_g , in the lamellar microdomain morphology varies, according to Semenov,² in the infinite molecular weight limit as $aN^{2/3}\chi^{1/6}$, where a is the statistical segment length, χ is the Flory–Huggins interaction parameter, and N is the number of segments in the chain. In the finite molecular weight case Helfand et al.³ have shown this to be modified to $aN^{9/14}\chi^{1/7}$. For an unperturbed polymer chain in the bulk, the root mean square radius of gyration, $R_{g,0}$, is given by $aN^{1/2}$. Thus, the ratio of the two reflects the extent to which the polymer chains are stretched, namely, $(\chi N)^{1/6}$ in the former case and $(\chi N)^{1/7}$ in the latter. As an example, for $\chi = 0.037$ and $N = 838$ extension ratios of 1.77 and 1.63 are predicted, respectively. For the stronger segregation case where $\chi = 0.11$ and $N = 610$ the predicted values are 2.02 and 1.82.

Attempts have been made experimentally to assess the extent of chain stretching parallel and perpendicular to the lamellar period. The simplest means by which this can be done is the direct measurement of the lamellar period. However, the measurement of the period is not

sufficient to determine the actual extent of chain stretching in both directions. Alternatively, by selectively labeling the blocks with deuterium, small-angle neutron scattering (SANS) has been used to determine the radius of gyration parallel and perpendicular to the lamellar period.^{4–7} Using highly oriented, macroscopic specimens of symmetric diblock copolymers with the incident neutron beam normal to the lamellar surfaces, the radius of gyration parallel to the lamellar surface can be obtained with ease. In such cases, using x to denote this direction, it is found that $R_{g,x} \simeq 0.7R_{g,0}$. However, SANS is not suitable for measurement of the radius of gyration perpendicular to the lamellar surface because of the interferences arising from the periodic lamellar microdomain structure. The measurement of the radius of gyration, $R_{g,z}$, normal to the lamellar microdomains, i.e., in the z direction, is not straightforward. In addition to the single-chain scattering, there is an intense component to the scattering arising from interferences between the lamellar microdomains. It is most difficult to eliminate this contribution to the scattering even by contrast matching⁸ techniques and, as of yet, no such measurements to measure $R_{g,z}$ have met with great success.

It has been shown previously for symmetric diblock copolymers of polystyrene (PS) and poly(methyl methacrylate) (PMMA) on silicon that the specific interactions of the PMMA block with the substrate and the lower surface energy of PS induce an orientation of the lamellar microdomain morphology parallel to the surface of the substrate.^{9–11} Neutron reflectivity studies have shown that the orientation persists over very large distances and, to within experimental errors, is essentially parallel to the surface of the substrate.^{9,10} This orientation has been found with both silicon and gold substrates.¹² Consequently, if the copolymer chains are stretched at the interface between the lamellae, they are stretched with respect to the surface of the specimen. Therefore, the copolymer films will be isotropic in the plane of the film but anisotropic normal to the surface. Optical waveguide techniques are sensitive to this birefringence and provide a unique means of accessing the chain extension at the interface. Recently, Lodge and Fredrickson¹³ reported

* To whom correspondence should be sent.

[†] Permanent address: Department of Polymer Science and Engineering, Sungkyunkwan University, Suwon, South Korea.

[‡] Permanent address: Department of Polymer Science and Engineering, Inha University, Incheon, South Korea.

• Abstract published in *Advance ACS Abstracts*, August 15, 1993.

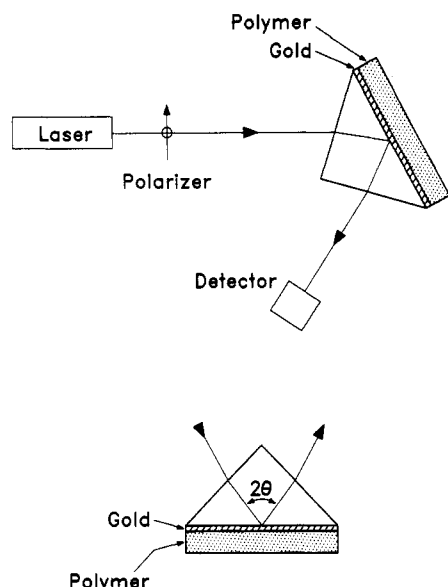


Figure 1. Schematic diagram of the attenuated total reflection waveguide geometry. Light from a laser polarized parallel or perpendicular to the plane of incidence passes through a prism and is reflected at a 500-Å layer of gold. The evanescent wave of the light extends beyond the gold layer and is guided in the polymer film at specific internal angles of incidence, θ , depending upon the refractive index and thickness of the film.

on the theoretical expressions for the static intrinsic birefringence for the lamellar diblock copolymers. In this study an optical waveguide technique is employed to measure the chain extension normal to the interface between the lamellar microdomains, and the experimental results are compared with these theoretical predictions.

Experimental Section

Experiments were performed on two symmetric diblock copolymers. The first was a symmetric block copolymer of PS and poly(2-vinylpyridine) (P2VP), denoted P(S-*b*-2VP), having a total molecular weight of 64 000 ($M_w/M_n = 1.02$) with a PS fraction of 0.5. The second was a diblock copolymer of PS and PMMA, denoted P(S-*b*-MMA), with a total molecular weight of 88 800 ($M_w/M_n = 1.03$) and PS fraction of 0.49. The P(S-*b*-MMA), purchased from Polymer Laboratories, was purified by extraction of the PS homopolymer with cyclohexane. Solutions of P(S-*b*-2VP) were prepared in *N,N*-dimethylformamide and solutions of P(S-*b*-MMA) in toluene. Solutions were filtered through a 1- μ m pore filter and spin-coated onto a gold-coated LaSF prism. Uniform films with thicknesses ranging from 1.5×10^8 to 20.0×10^8 Å were prepared by varying the speed of the spinner and/or varying the concentration of the copolymer. Samples were annealed in vacuum at 170 °C for the desired period of time. Birefringence results are reported only for films with a thickness of $\sim 9 \times 10^8$ Å since the results were found to be independent of film thickness.

The films were characterized using attenuated total reflectance (ATR) spectroscopy of the waveguide modes as shown schematically in Figure 1.¹⁴ Light, polarized parallel or perpendicular to the surface of the film, from a He-Ne laser ($\lambda = 6328$ Å) impinges on the surface of a LaSF prism and then onto the prism/gold interface at an internal angle θ . The intensity reflected from the surface at the corresponding angle is measured with a photodiode detector scanning at 2θ . Depending upon the refractive index of the film and its thickness, light will be guided into the copolymer film at discrete angles. A typical profile for the P(S-*b*-2VP) annealed for 140 h at 170 °C is shown in Figure 2. The positions of the minima are well resolved and, by use of Fresnel formalism, these can be fitted to yield the thickness and refractive indices. As can be seen in Figure 2, the theoretically calculated curve (dashed line) accurately determines the positions of the minima in the experimental data (solid line). Instrumental broadening was not taken into account in the calculated profile

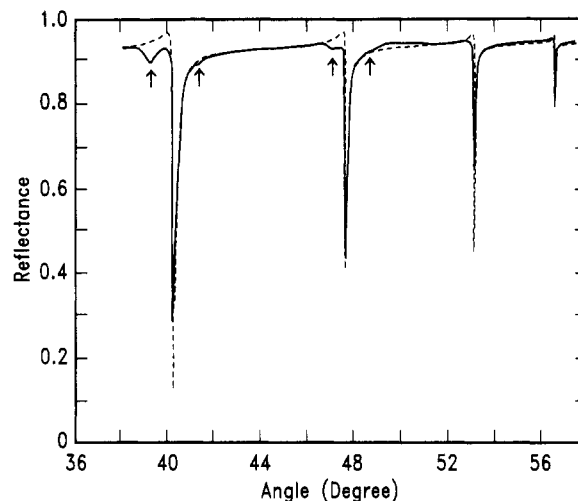


Figure 2. Intensity of light reflected from the gold surface as a function of the internal incidence angle θ . In this case the light was polarized parallel to the film surface (perpendicular to the plane of incidence). The P(S-*b*-2VP) copolymer was annealed for 140 h at 170 °C and measured at 23 °C. The dashed line is the calculated profile used to fit the positions of the minima in the experimental profile.

Table I. ATR Results on P(S-*b*-2VP)^a

annealing time (h)	measd at (°C)	thickness ^b (nm)	refractive indices		birefringence $\Delta_T = n_{\perp} - n_{\parallel}$
			n_{\perp}	n_{\parallel}	
0	23	1143	1.5846	1.5820	0.0026
20	23	1109	1.5881	1.5883	-0.0002
140	23	1111	1.5879	1.5881	-0.0002
140	100	1175	1.5765	1.5772	-0.0007
140	139	1199	1.5642	1.5648	-0.0006
140	168	1204	1.5547	1.5554	-0.0007
140	178	1211	1.5517	1.5524	-0.0007

^a The gold layer was 46.75 nm thick. ^b The change in the film thickness with temperature is consistent with the thermal expansion coefficient of the polymer.

Table II. ATR Results on P(S-*b*-MMA)^a

annealing time (h)	measd at (°C)	thickness (nm)	refractive indices		birefringence $\Delta_T = n_{\perp} - n_{\parallel}$
			n_{\perp}	n_{\parallel}	
0	23	934	1.5364	1.5336	0.0028
112	23	902	1.5323	1.5341	-0.0018
277	23	907	1.5319	1.5343	-0.0024
341	23	905	1.5327	1.5345	-0.0018
505	23	906	1.5325	1.5342	-0.0017

^a The gold layer was 50.61 nm thick.

which accounts for some of the broadening. In this manner, the ordinary (n_{\parallel}) and extraordinary (n_{\perp}) refractive indices and the film thickness can be determined, thereby yielding the total birefringence, $\Delta_T = n_{\perp} - n_{\parallel}$, of the copolymer films. To obtain these three parameters accurately, at least three waveguide modes must be measured.

Results and Discussion

A compilation of the film thickness and refractive indices parallel and perpendicular to the surfaces of the specimens are shown in Tables I and II. The data shown are for the as-cast specimens followed by successive annealings at 170 °C for the times specified. It is first noticed that the film thickness decreases by nearly 2.9% for P(S-*b*-VP) and 3.5% for P(S-*b*-MMA) upon the initial annealing. This can be attributed to a loss of residual solvent and a densification of the film during the first heating. Subsequent annealing showed no change in the film thickness. For the as-cast specimens of both P(S-*b*-2VP) and P(S-*b*-MMA), it is found that $n_{\parallel} < n_{\perp}$, i.e., $\Delta_T > 0$, indicating that the solvent-casting process, as expected, orients the

copolymer chains, on average, parallel to the film surface. This is similar to the results of Prest and Luca, who found, for the solvent-cast film of PS, that the PS chains were oriented parallel to the film surface.¹⁵ However, the presence of solvent and stresses induced during drying makes it difficult to determine accurately the extent of orientation. It is also expected that the rotation speed at which the specimens are prepared will alter the orientation of the copolymer chains. However, this was not investigated here since this represented a nonequilibrium state. While the film thickness decreases upon the initial heating and remains constant with further annealing, the birefringence changes sign and becomes negative on the order of $-(7 \pm 1) \times 10^{-4}$ and $-(20 \pm 1) \times 10^{-4}$ for P(S-*b*-2VP) and P(S-*b*-MMA), respectively, and changes little with further annealing. This suggests that upon annealing the chains become oriented perpendicular to the film surface. This is consistent with the orientation of the lamellar microdomains parallel to the film surface forming a multilayered structure since the copolymer chains will be oriented normal to the interface between the lamellar microdomains.

The first question to be asked is whether or not the lamellar microdomains are oriented parallel to the film surface. Independent dynamic secondary ion mass spectrometry studies performed on the same P(S-*b*-MMA) used in this study with an Ar⁺ ion beam showed a clear periodic oscillation characteristic of the lamellar microdomain orientation parallel to the film surface with PS located preferentially at both the Au and air interfaces. The same applies to P(S-*b*-2VP). However, the 2VP block is preferentially located at the Au interface and the PS at the air surface.¹⁶ In fact, for the P(S-*b*-2VP) the tendency to form a multilayered morphology is stronger. The χ between PS and PMMA at 170 °C is 0.037;¹⁷ thus $\chi N = 31.0$ for P(S-*b*-MMA) used in this study. The χ between PS and P2VP at 170 °C is 0.11;¹⁸ thus $\chi N = 67.1$ for P(S-*b*-2VP) used in this study. This, coupled with the preferential interaction of P2VP with the Au would result in a stronger tendency to form multilayers. The larger value of χN for P(S-*b*-2VP) would mean a stronger microphase separation.¹¹ Therefore, we can assume that the lamellar microdomains are also oriented parallel to the film surface for P(S-*b*-2VP). In addition to this, at the perimeter of both the P(S-*b*-MMA) and P(S-*b*-2VP) samples, optical microscopic observations show a clear terracing on the surface which is a direct ramification of the multilayered structure.

For multilayered specimens where one component preferentially resides at both the air/polymer and polymer/substrate interfaces, as is the case here for P(S-*b*-MMA), the thickness at any point is given by nL , where n is an integer and L is the lamellar period.¹² Previous neutron reflectivity¹⁰ measurements have shown that the period, L , for this copolymer is ~ 38 nm. This, for the specimens measured here with a total thickness of 904 ± 2 nm, means that this specimen is comprised of 24 periods with each period being 37.6 ± 0.1 nm, which agrees well with the reflectivity results. In the case of P(S-*b*-2VP), where PS preferentially resides at the air surface and P2VP at the Au interface, thickness at any point should be given by $(n + 0.5)L$. For the P(S-*b*-2VP) studied here, independent small-angle X-ray scattering studies yielded a lamellar period of 39 nm. Using this value for each period, with $n = 28$, i.e., 28.5 copolymer periods in the film, the specimen's thickness is 1111 nm. The total thickness measured for this specimen was 1110 ± 2 nm, which is in excellent agreement.

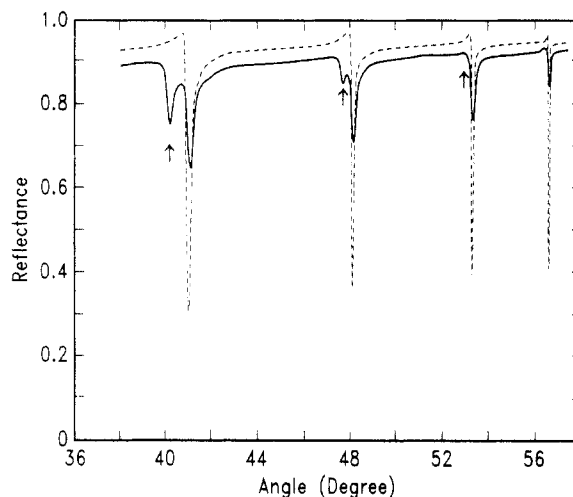


Figure 3. Intensity of reflected light from the gold surface as a function of the internal incidence angle θ for the same sample as shown in Figure 2, only changing the position of the spot where the measurements were taken. The arrows indicate the pronounced shoulders that can be seen. The appearance of the two sets of minima is characteristic of a film with two discrete thicknesses.

An equally compelling argument that the multilayered structure is formed can be made by observing the shape of the ATR profiles. It is noticed in Figure 2 that, in addition to the strong modes characteristic of the bulk of the film, in the first and second modes, two distinct subsidiary minima, marked with arrows, are observed. It will be recalled that, by the nature of the surface-induced orientation of the symmetric diblock copolymers, if the initial thickness of the specimen is not precisely $(n + 0.5)L$ for P(S-*b*-2VP) or nL for P(S-*b*-MMA), then either islands or holes will be formed on the surface of the film. The heights of these islands or holes will be precisely L . Optical microscopy studies^{11,19} and atomic force microscopy²⁰ studies show this effect quite clearly, and hence the phenomenon is well documented. For the ATR studies here, this means that the presence of islands or holes will effectively be seen as films with the identical optical properties but with thickness differing by L . Therefore, the minimum appearing on the left of the main mode would represent the presence of holes, and islands would be responsible for the right minimum. These subsidiary minima were not observed for the as-cast specimens but became distinct upon annealing. This observation supports our interpretation. Much stronger evidence supporting this interpretation can be found in Figure 3, which is the result of the measurements taken at a different spot of the same P(S-*b*-2VP) specimen as used for the measurements shown in Figure 2. By comparing Figure 3 with Figure 2, it will clearly be noticed that the strong modes shown in Figure 2 are also observed in Figure 3 at the same positions (marked with arrows) but Figure 3 exhibits other strong modes not observed in Figure 2. These additional strong modes are due to islands with a height of L . Analyzing these subsidiary maxima as main modes yields a thickness of 1141 nm. Taking the difference between this value and the dominant thickness of the film yields a value of 31 ± 2 nm for the step height, which is in reasonable agreement with the value determined from X-ray scattering measurements. In the case of P(S-*b*-MMA), such sharp additional peaks were not observed; instead in the first and second modes either subsidiary minima with diminished peak intensities or pronounced shoulders were observed. However, in a manner identical to the calculations done for P(S-*b*-2VP), thicknesses ranging from 867 to 873 nm were found for P(S-*b*-MMA).

The difference between these values and the dominant thickness of the film gives a value of 35 ± 3 nm for the step height, which corresponds quite well to the expected value of 37.6 nm. A more precise definition of the step height would require a detailed decomposition of the ATR profile, which was not performed here. However, the experimental observation of these additional minima and the good agreement between the measured and expected heights suggest that the ordering has propagated through both copolymer films. Direct observation of the formation of islands in the center of this sample by optical microscopy was not possible due to the thickness of the specimens.

The total birefringence of a sample is given by

$$\Delta_T = \Delta_D + \Delta_F + \Delta_I \quad (1)$$

where Δ_D is the deformation birefringence, Δ_F is the form birefringence, and Δ_I is the intrinsic birefringence. The deformation birefringence arises from bond angle distortions to the backbones and pendant groups during the orientation of the chain. For most polymers above the glass transition temperature, T_g , the deformation birefringence is small even with the chains being elongated substantially and can be neglected. Even for diblock copolymers, when the measurements are performed above the T_g of the component blocks, Δ_D should be negligible if the extension ratios are not substantial and the strain induced by thermal expansion is small. However, when the specimen is cooled from higher temperatures to below T_g and the measurements are performed at temperatures lower than T_g , the situation will be quite different, especially for the specimen having the geometry studied here where the copolymer is confined on a substrate. The thermal expansion coefficients for PS and PMMA²¹ for temperatures lower than T_g are essentially equal at $\sim 7 \times 10^{-5}$ K⁻¹. P2VP was assumed to have a thermal expansion coefficient not much different from that of PS or PMMA. On the other hand, the LaSF substrate²² has a thermal expansion coefficient of $\sim 7 \times 10^{-6}$ K⁻¹, an order of magnitude less than that of the copolymer. Thus, when the specimen is cooled from above to below T_g , in comparison to the substrate, the copolymer chains contract significantly. The strong attachment of the copolymers to the substrate essentially strains the copolymer parallel to the substrate surface and the resulting Δ_D will contribute positively in its value to Δ_T . This strain is not reflected in a distortion of the lamellar microdomain morphology since neutron reflectivity measurements have shown that the morphology is basically unchanged over a temperature range from room temperature up to ~ 170 °C.²³ Consequently, the imposed strain must result in distortions to the monomer units and cause the Δ_D to be significant in magnitude. This argument can easily be validated when analyzing the ATR results of P(S-*b*-2VP) given in Table I. The value of Δ_T is $-(2 \pm 1) \times 10^{-4}$ at 25 °C where Δ_D would be significant and changes to $-(7 \pm 1) \times 10^{-4}$ above 100 °C where Δ_D would be negligible. Therefore, we conclude that the strain resulting from the copolymer contraction has caused a Δ_D of $\sim 5 \times 10^{-4}$. From the above discussion, it is evident that measurements must be performed at elevated temperatures where the contribution of Δ_D would be minimized.

For a series of platelets comprised of two different materials, A and B, as is the case here for a multilayer of diblock copolymer having lamellar microdomains oriented parallel to the substrate surface, the form birefringence

is given by²⁴

$$\Delta_F = \frac{n_A n_B}{(\phi_A n_B^2 + \phi_B n_A^2)^{0.5}} - (\phi_A n_A^2 + \phi_B n_B^2)^{0.5} \quad (2)$$

where ϕ_i is the volume fraction of phase *i* with refractive index n_i . With $n_{PS} = 1.595$, $n_{P2VP} = 1.620$, and $\phi_{PS} = 0.50$, $\Delta_F = -2 \times 10^{-4}$ for P(S-*b*-2VP). Using $n_{PS} = 1.595$, $n_{PMMA} = 1.490$, and $\phi_{PS} = 0.49$, $\Delta_F = -36 \times 10^{-4}$ for P(S-*b*-MMA). These values of Δ_F represent upper limits of Δ_F for each copolymer since eq 2 is valid only for a system with infinitely sharp phase boundaries. However, for block copolymers there exist interphase regions where the two dissimilar segments are mixed, which will tend to reduce Δ_F . Previous studies showed that the width of the interface between the PS and PMMA microdomains is 50 ± 2 Å.^{9,10} Since there are two interfaces per period L ($=37.6$ nm), then $\sim 27\%$ of the material resides within the interface, which could reduce Δ_F for P(S-*b*-MMA) to -26×10^{-4} . In the case of P(S-*b*-2VP), the width of the interface is expected to be much narrower because of the greater value of χN . Moreover, the refractive indices measured in this study are accurate only within $\pm 1 \times 10^{-4}$, and the expected value of Δ_F for P(S-*b*-VP) is -2×10^{-4} without considering the presence of interface. Therefore, it will be assumed that Δ_F for P(S-*b*-2VP) is -2×10^{-4} .

The only remaining contribution to the total birefringence is the intrinsic birefringence which is related to the extent of chain stretching at the interface. It was shown that Δ_D is $\sim 5 \times 10^{-4}$ for the geometry employed here for $T < T_g$, which is the case for the results on P(S-*b*-MMA). Δ_D should be negligible above T_g , which is the case here for the results on P(S-*b*-2VP) above 100 °C. The expected value of Δ_F is -2×10^{-4} for P(S-*b*-2VP) and -26×10^{-4} for P(S-*b*-MMA). Experimentally, Δ_T was found to be -7×10^{-4} for P(S-*b*-2VP) when the measurements were performed at above 100 °C. Therefore, using eq 1, Δ_I is found to be -5×10^{-4} for P(S-*b*-2VP). Similarly, the value of Δ_I is 1×10^{-4} for P(S-*b*-MMA).

Recently, Lodge and Fredrickson¹³ reported the theoretical expressions for the static intrinsic birefringence for lamellar block copolymers. We can use their expression to deduce the extent of chain stretching from the intrinsic birefringence. The intrinsic birefringence is given by

$$\Delta_I = \left(\frac{\pi^3}{90} \right) (N_A) \left(\frac{M_A}{\rho_A} + \frac{M_B}{\rho_B} \right)^{-1} \times \left\{ \frac{(n_A^2 + 2)^2}{n_A} (\alpha_1 - \alpha_2)_A \left(\frac{L_A}{r_{0,A}} \right)^2 + \frac{(n_B^2 + 2)^2}{n_B} (\alpha_1 - \alpha_2)_B \left(\frac{L_B}{r_{0,B}} \right)^2 \right\} \quad (3)$$

where N_A is Avogadro's number and M_i is the molecular weight of block *i* with density ρ_i and refractive index n_i . α_1 and α_2 are the polarizability parallel to and normal to the segment axis, respectively. L_i and $r_{0,i}$ denote the layer thickness and the root mean square unperturbed end-to-end distance of block *i*, respectively. Using eq 3 together with the experimentally measured value of Δ_I , the ratio $L_i/r_{0,i}$ can be obtained and will indicate the extent of chain stretching at the interface. For P(S-*b*-2VP) it was assumed that $L_{PS}/r_{0,PS} = L_{P2VP}/r_{0,P2VP}$. Since $r_{0,i}^2 = 6R_{g,i}^2$, then, from eq 3, $\Delta_I = (-2.1 \times 10^{-4})(L^2/R_{g,0}^2)$. For this calculation, $(\alpha_1 - \alpha_2) = -1.5 \times 10^{-23}$ was used for both PS and P2VP. From the above relationship and the experimentally determined value of -5×10^{-4} for Δ_I , $L/R_{g,0}$ is found to be 1.51 for P(S-*b*-2VP). In the case of P(S-*b*-MMA), the previously reported²⁵ values for $L_i/R_{g,0,i}$ (1.59 for PS block

and 1.55 for PMMA block), with $(\alpha_1 - \alpha_2) = 1.6 \times 10^{-24}$ for PMMA, were put into eq 3 and the resulting calculated value of -1.7×10^{-4} was found for Δ_I . To within the error limits of the measurements, this agrees very well with the experimental value of $\pm 1 \times 10^{-4}$.

Conclusion

Thin films of two symmetric diblock copolymers, P(S-*b*-2VP) and P(S-*b*-MMA), were characterized using attenuated total reflectance spectroscopy to investigate the extent of chain stretching at the interface. In the case of P(S-*b*-MMA), $\Delta_F = -26 \times 10^{-4}$ and $\Delta_I = -1.7 \times 10^{-4}$, demonstrating that Δ_F contributes significantly to Δ_T . In fact, for highly oriented styrene-butadiene diblock copolymers with a cylindrical morphology, Keller and co-workers²⁶ found that Δ_F dominated Δ_T . In the case of P(S-*b*-2VP), $\Delta_F = -2 \times 10^{-4}$ and $\Delta_I = -5 \times 10^{-4}$. Here, the extent of chain stretching, given by $L/R_{g,0}$, is found to be 1.51 for P(S-*b*-2VP). This is lower than the value of 2.02 predicted by Semenov and 1.82 predicted by Helfand et al. in the strong segregation limit. In these cases, Δ_I should have been -9×10^{-4} and -7×10^{-4} for each case, respectively. Since the measured value is accurate only to within $\pm 1 \times 10^{-4}$, the deviation from Helfand's prediction is within experimental uncertainties.

Acknowledgment. The authors would like to thank V. R. Deline for assistance with the dynamic SIMS measurements, K. Shull for valuable discussions, and D. Y. Yoon for his critical comments. We also express our appreciation to IBM-Korea and KOSEF for the support of J.K. and I.C. during their visits to the IBM Almaden Research Center. This work was supported, in part, by the Department of Energy, Office of Basic Energy Sciences, under Contract DE-FG03-88ER45375. J.W.M. acknowledges, with gratitude, financial support from the National Science Foundation (Grant CTS-9107025).

References and Notes

- (1) See, for example: *Developments in Block Copolymers—1*; Goodman, I., Ed.; Applied Science Publishers: New York, 1985.
- (2) Semenov, A. N. *Sov. Phys.—JETP (Engl. Transl.)* **1985**, *61*, 733.
- (3) Helfand, G.; Fredrickson, G. H. *J. Chem. Phys.* **1987**, *87*, 6.
- (4) Hadziioannou, G.; Picot, C.; Skoulios, A.; Ionescu, M.-L.; Mathis, A.; Duplessix, R.; Gallot, Y.; Lingelser, J.-P. *Macromolecules* **1982**, *15*, 263.
- (5) Hasegawa, H.; Hashimoto, T.; Kawai, H.; Lodge, T. P.; Amis, E. J.; Glinka, C. J.; Han, C. C. *Macromolecules* **1985**, *18*, 67.
- (6) Hasegawa, H.; Tanaka, H.; Hashimoto, T.; Han, C. C. *Macromolecules* **1987**, *20*, 2120.
- (7) Matsushita, Y.; Mori, K.; Saguchi, R.; Noda, I.; Nagasawa, M.; Chang, T.; Glinka, C. J.; Han, C. C. *Macromolecules* **1990**, *23*, 4387.
- (8) Quan, X.; Koberstein, J. T. *J. Polym. Sci., Polym. Phys. Ed.* **1987**, *25*, 2381.
- (9) Anastasiadis, S. H.; Russell, T. P.; Satija, S. K.; Majkrzak, C. F. *Phys. Rev. Lett.* **1989**, *62*, 1852.
- (10) Anastasiadis, S. H.; Russell, T. P.; Satija, S. K.; Majkrzak, C. F. *J. Chem. Phys.* **1990**, *92*, 5677.
- (11) Coulon, G.; Russell, T. P.; Deline, V. R.; Green, P. F. *Macromolecules* **1989**, *22*, 2581.
- (12) Russell, T. P.; Coulon, G.; Deline, V. R.; Miller, D. C. *Macromolecules* **1989**, *22*, 4600.
- (13) Lodge, T. P.; Fredrickson, G. H. *Macromolecules* **1992**, *25*, 5643.
- (14) Herminghaus, S.; Smith, B. A.; Swalen, J. D. *Macromolecules*, in press.
- (15) Prest, W. M.; Luca, D. J. *J. Appl. Phys.* **1979**, *50*, 6062.
- (16) Shull, K.; Saurel, B., unpublished results. The surface tension of PS was found to be 32 dyn/cm while that of P2VP was found to be 36 dyn/cm. However, when P(S-*b*-2VP) is cast on the gold substrate, P2VP instead of PS always resides at the gold surface. The origin for this observation is not clear yet.
- (17) Russell, T. P.; Hjelm, R. P.; Seeger, P. *Macromolecules* **1990**, *23*, 890.
- (18) Shull, K.; Saurel, B., unpublished results.
- (19) Coulon, G.; Collin, B.; Ausserre, D.; Chatenay, D.; Russell, T. P. *J. Phys.* **1990**, *51*, 2801.
- (20) Maaloum, M.; Ausserre, D.; Chatenay, D.; Coulon, G.; Gallot, Y. *J. Phys. (Paris)*, submitted.
- (21) Brandrup, J.; Immergut, I. *Polymer Handbook*; John Wiley and Sons: New York, 1975.
- (22) Ohara Optical Glass, LASF08 specifications.
- (23) Mayes, A. M.; Russell, T. P., unpublished results.
- (24) Born, M.; Wolf, E. *Principles of Optics*; Pergamon: New York, 1970.
- (25) Mayes, A. M.; Russell, T. P.; Satija, S. K.; Majkrzak, C. F. *Macromolecules* **1992**, *25*, 6523.
- (26) Keller, A.; Dlugosz, J.; Folkes, M. J.; Pedemonte, E.; Scalisi, F. P.; Willmouth, F. M. *J. Phys. (Paris)* **1971**, *65*, 295.